Extracting and Composing Robust Features with Denoising Autoencoders

Pascal Vincent,
Hugo Larochelle, Yoshua Bengio, Pierre-Antoine Manzagol

Université de Montréal, LISA Lab

July 2008

The problem

- Building good predictors on complex domains means learning complicated functions.
- These are best represented by multiple levels of non-linear operations i.e. deep architectures.
- Deep architectures are an old idea: multi-layer perceptrons.
- Learning the parameters of deep architectures proved to be challenging!

Training deep architectures: attempted solutions

- **Solution 1**: initialize at random, and do gradient descent (Rumelhart, Hinton and Williams, 1986).
  → disappointing performance. Stuck in poor solutions.

- **Solution 2**: Deep Belief Nets (Hinton, Osindero and Teh, 2006): initialize by stacking Restricted Boltzmann Machines, fine-tune with Up-Down.
  → impressive performance.

  Key seems to be good unsupervised layer-by-layer initialization...

- **Solution 3**: initialize by stacking autoencoders, fine-tune with gradient descent. (Bengio et al., 2007; Ranzato et al., 2007)
  → Simple generic procedure, no sampling required.
  Performance almost as good as Solution 2

...but not quite. Can we do better?

Training deep architectures: attempted solutions

- **Solution 1**: initialize at random, and do gradient descent (Rumelhart, Hinton and Williams, 1986).
  → disappointing performance. Stuck in poor solutions.

- **Solution 2**: Deep Belief Nets (Hinton, Osindero and Teh, 2006): initialize by stacking Restricted Boltzmann Machines, fine-tune with Up-Down.
  → impressive performance.

  Key seems to be good unsupervised layer-by-layer initialization. . .

- **Solution 3**: initialize by stacking autoencoders, fine-tune with gradient descent. (Bengio et al., 2007; Ranzato et al., 2007)
  → Simple generic procedure, no sampling required.
  Performance almost as good as Solution 2

. . . but not quite. Can we do better?

Training deep architectures: attempted solutions

- **Solution 1**: initialize at random, and do gradient descent (Rumelhart, Hinton and Williams, 1986).
  $\longrightarrow$ disappointing performance. Stuck in poor solutions.
- **Solution 2**: Deep Belief Nets (Hinton, Osindero and Teh, 2006): initialize by stacking Restricted Boltzmann Machines, fine-tune with Up-Down.
  $\longrightarrow$ impressive performance.

  Key seems to be good unsupervised layer-by-layer initialization...
- **Solution 3**: initialize by stacking autoencoders, fine-tune with gradient descent. (Bengio et al., 2007; Ranzato et al., 2007)
  $\longrightarrow$ Simple generic procedure, no sampling required.
  Performance almost as good as Solution 2

...but not quite. Can we do better?

Training deep architectures: attempted solutions

- **Solution 1**: initialize at random, and do gradient descent (Rumelhart, Hinton and Williams, 1986).
  → disappointing performance. Stuck in poor solutions.
- **Solution 2**: Deep Belief Nets (Hinton, Osindero and Teh, 2006): initialize by stacking Restricted Boltzmann Machines, fine-tune with Up-Down.
  → impressive performance.

  Key seems to be good unsupervised layer-by-layer initialization...
- **Solution 3**: initialize by stacking autoencoders, fine-tune with gradient descent. (Bengio et al., 2007; Ranzato et al., 2007)
  → Simple generic procedure, no sampling required.
  Performance almost as good as Solution 2

...but not quite. Can we do better?

Can we do better?

Open question: what would make a good unsupervised criterion for finding good initial intermediate representations?

- Inspiration: our ability to "fill-in-the-blanks" in sensory input.
  missing pixels, small occlusions, image from sound, ...
- Good fill-in-the-blanks performance $\leftrightarrow$ distribution is well captured.
- $\rightarrow$ old notion of associative memory (motivated Hopfield models (Hopfield, 1982))

What we propose:
unsupervised initialization by explicit fill-in-the-blanks training.

The denoising autoencoder

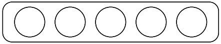

$\mathbf{x}$

- Clean input $\mathbf{x} \in [0,1]^d$ is partially destroyed, yielding corrupted input: $\tilde{\mathbf{x}} \sim q_{\mathcal{D}}(\tilde{\mathbf{x}}|\mathbf{x})$.
- $\tilde{\mathbf{x}}$ is mapped to hidden representation $\mathbf{y} = f_\theta(\tilde{\mathbf{x}})$.
- From $\mathbf{y}$ we reconstruct a $\mathbf{z} = g_{\theta'}(\mathbf{y})$.
- Train parameters to minimize the cross-entropy "reconstruction error" $L_{\mathbb{H}}(\mathbf{x}, \mathbf{z}) = \mathbb{H}(\mathcal{B}_{\mathbf{x}} \| \mathcal{B}_{\mathbf{z}})$, where $\mathcal{B}_{\mathbf{x}}$ denotes multivariate Bernoulli distribution with parameter $\mathbf{x}$.

The denoising autoencoder

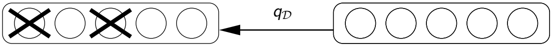

- Clean input $\mathbf{x} \in [0,1]^d$ is partially destroyed, yielding corrupted input: $\tilde{\mathbf{x}} \sim q_{\mathcal{D}}(\tilde{\mathbf{x}}|\mathbf{x})$.
- $\tilde{\mathbf{x}}$ is mapped to hidden representation $\mathbf{y} = f_\theta(\tilde{\mathbf{x}})$.
- From $\mathbf{y}$ we reconstruct a $\mathbf{z} = g_{\theta'}(\mathbf{y})$.
- Train parameters to minimize the cross-entropy "reconstruction error" $L_{\mathbb{H}}(\mathbf{x}, \mathbf{z}) = \mathbb{H}(\mathcal{B}_{\mathbf{x}} \| \mathcal{B}_{\mathbf{z}})$, where $\mathcal{B}_{\mathbf{x}}$ denotes multivariate Bernoulli distribution with parameter $\mathbf{x}$.

The denoising autoencoder

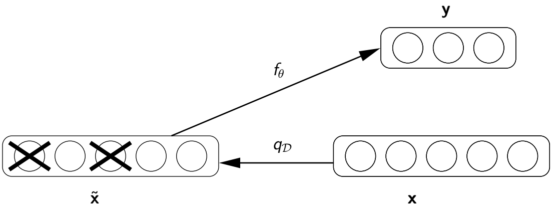

- Clean input $\mathbf{x} \in [0,1]^d$ is partially destroyed, yielding corrupted input: $\tilde{\mathbf{x}} \sim q_\mathcal{D}(\tilde{\mathbf{x}}|\mathbf{x})$.
- $\tilde{\mathbf{x}}$ is mapped to hidden representation $\mathbf{y} = f_\theta(\tilde{\mathbf{x}})$.
- From $\mathbf{y}$ we reconstruct a $\mathbf{z} = g_{\theta'}(\mathbf{y})$.
- Train parameters to minimize the cross-entropy "reconstruction error" $L_{\mathbb{H}}(\mathbf{x}, \mathbf{z}) = \mathbb{H}(\mathcal{B}_\mathbf{x} \| \mathcal{B}_\mathbf{z})$, where $\mathcal{B}_\mathbf{x}$ denotes multivariate Bernoulli distribution with parameter $\mathbf{x}$.

The denoising autoencoder

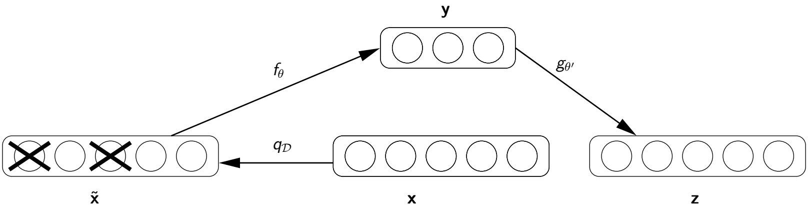

- Clean input $\mathbf{x} \in [0,1]^d$ is partially destroyed, yielding corrupted input: $\tilde{\mathbf{x}} \sim q_{\mathcal{D}}(\tilde{\mathbf{x}}|\mathbf{x})$.
- $\tilde{\mathbf{x}}$ is mapped to hidden representation $\mathbf{y} = f_\theta(\tilde{\mathbf{x}})$.
- From $\mathbf{y}$ we reconstruct a $\mathbf{z} = g_{\theta'}(\mathbf{y})$.
- Train parameters to minimize the cross-entropy "reconstruction error" $L_{\mathbb{H}}(\mathbf{x}, \mathbf{z}) = \mathbb{H}(\mathcal{B}_{\mathbf{x}} \| \mathcal{B}_{\mathbf{z}})$, where $\mathcal{B}_{\mathbf{x}}$ denotes multivariate Bernoulli distribution with parameter $\mathbf{x}$.

The denoising autoencoder

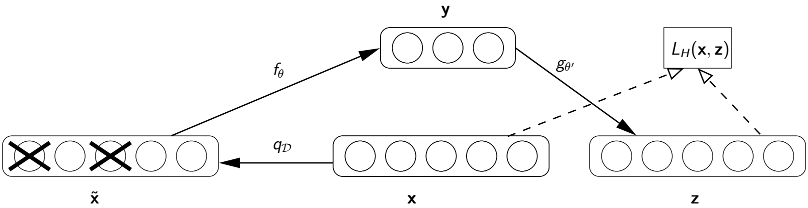

- Clean input $\mathbf{x} \in [0, 1]^d$ is partially destroyed, yielding corrupted input: $\tilde{\mathbf{x}} \sim q_{\mathcal{D}}(\tilde{\mathbf{x}}|\mathbf{x})$.
- $\tilde{\mathbf{x}}$ is mapped to hidden representation $\mathbf{y} = f_\theta(\tilde{\mathbf{x}})$.
- From $\mathbf{y}$ we reconstruct a $\mathbf{z} = g_{\theta'}(\mathbf{y})$.
- Train parameters to minimize the cross-entropy "reconstruction error" $L_{\mathbb{H}}(\mathbf{x}, \mathbf{z}) = \mathbb{H}(\mathcal{B}_{\mathbf{x}} \| \mathcal{B}_{\mathbf{z}})$, where $\mathcal{B}_{\mathbf{x}}$ denotes multivariate Bernoulli distribution with parameter $\mathbf{x}$.

The input corruption process $q_{\mathcal{D}}(\tilde{\mathbf{x}}|\mathbf{x})$

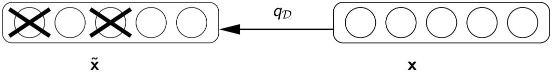

- Choose a fixed proportion ν of components of $\mathbf{x}$ at random.
- Reset their values to 0.
- Can be viewed as replacing a component considered missing by a default value.

Other corruption processes are possible.

Form of parameterized mappings

We use standard sigmoid network layers:

- $\mathbf{y} = f_\theta(\tilde{\mathbf{x}}) = \mathrm{sigmoid}(\underbrace{\mathbf{W}}_{d' \times d}\tilde{\mathbf{x}} + \underbrace{\mathbf{b}}_{d' \times 1})$
- $g_{\theta'}(\mathbf{y}) = \mathrm{sigmoid}(\underbrace{\mathbf{W}'}_{d \times d'}\mathbf{y} + \underbrace{\mathbf{b}'}_{d \times 1})$.

Denoising using classical autoencoders was actually introduced much earlier (LeCun, 1987; Gallinari et al., 1987), as an alternative to Hopfield networks (Hopfield, 1982).

Form of parameterized mappings

We use standard sigmoid network layers:

- $\mathbf{y} = f_\theta(\tilde{\mathbf{x}}) = \mathrm{sigmoid}(\underbrace{\mathbf{W}}_{d' \times d} \tilde{\mathbf{x}} + \underbrace{\mathbf{b}}_{d' \times 1})$
- $g_{\theta'}(\mathbf{y}) = \mathrm{sigmoid}(\underbrace{\mathbf{W}'}_{d \times d'} \mathbf{y} + \underbrace{\mathbf{b}'}_{d \times 1})$.

Denoising using classical autoencoders was actually introduced much earlier (LeCun, 1987; Gallinari et al., 1987), as an alternative to Hopfield networks (Hopfield, 1982).

Learning deep networks
Layer-wise initialization

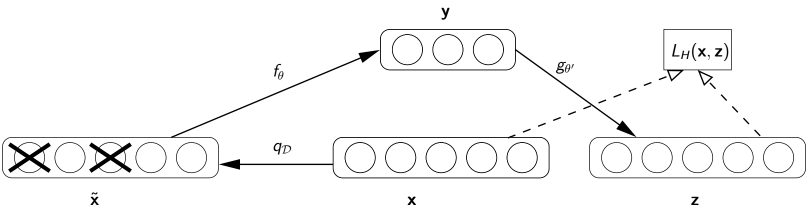

1. Learn first mapping f_θ by training as a denoising autoencoder.
2. Remove scaffolding. Use f_θ directly on input yielding higher level representation.
3. Learn next level mapping $f_\theta^{(2)}$ by training denoising autoencoder on current level representation.
4. Iterate to initialize subsequent layers.

Learning deep networks

Layer-wise initialization

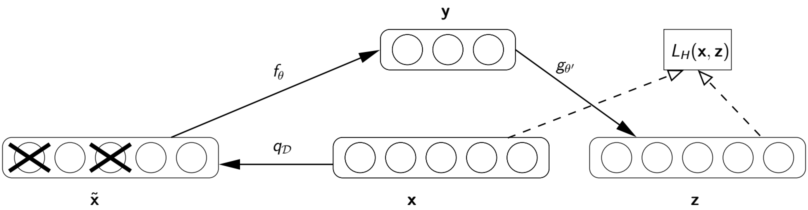

1. Learn first mapping f_θ by training as a denoising autoencoder.
2. Remove scaffolding. Use f_θ directly on input yielding higher level representation.
3. Learn next level mapping $f_\theta^{(2)}$ by training denoising autoencoder on current level representation.
4. Iterate to initialize subsequent layers.

Learning deep networks
Layer-wise initialization

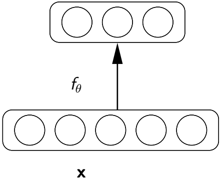

1. Learn first mapping f_θ by training as a denoising autoencoder.
2. Remove scaffolding. Use f_θ directly on input yielding higher level representation.
3. Learn next level mapping $f_\theta^{(2)}$ by training denoising autoencoder on current level representation.
4. Iterate to initialize subsequent layers.

Learning deep networks
Layer-wise initialization

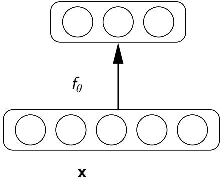

1. Learn first mapping f_θ by training as a denoising autoencoder.
2. Remove scaffolding. Use f_θ directly on input yielding higher level representation.
3. Learn next level mapping $f_\theta^{(2)}$ by training denoising autoencoder on current level representation.
4. Iterate to initialize subsequent layers.

Learning deep networks
Layer-wise initialization

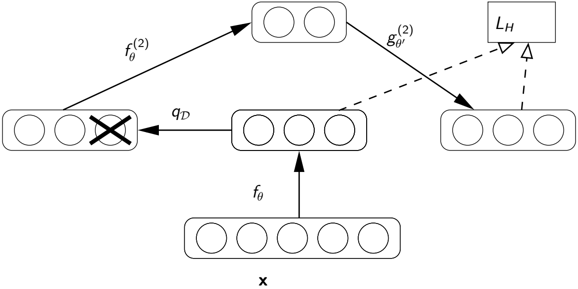

1. Learn first mapping f_θ by training as a denoising autoencoder.
2. Remove scaffolding. Use f_θ directly on input yielding higher level representation.
3. Learn next level mapping $f_\theta^{(2)}$ by training denoising autoencoder on current level representation.
4. Iterate to initialize subsequent layers.

Learning deep networks
Layer-wise initialization

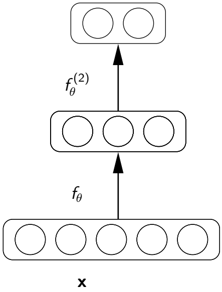

1. Learn first mapping f_θ by training as a denoising autoencoder.
2. Remove scaffolding. Use f_θ directly on input yielding higher level representation.
3. Learn next level mapping $f_\theta^{(2)}$ by training denoising autoencoder on current level representation.
4. Iterate to initialize subsequent layers.

Learning deep networks

Layer-wise initialization

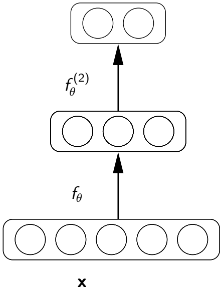

1. Learn first mapping f_θ by training as a denoising autoencoder.
2. Remove scaffolding. Use f_θ directly on input yielding higher level representation.
3. Learn next level mapping $f_\theta^{(2)}$ by training denoising autoencoder on current level representation.
4. Iterate to initialize subsequent layers.

Learning deep networks
Supervised fine-tuning

- Initial deep mapping was learnt in an unsupervised way.
- → initialization for a supervised task.
- Output layer gets added.
- Global fine tuning by gradient descent on supervised criterion.

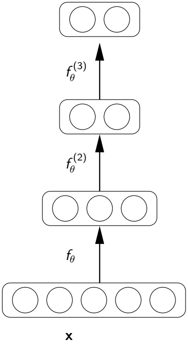

Learning deep networks
Supervised fine-tuning

- Initial deep mapping was learnt in an unsupervised way.
- $\rightarrow$ initialization for a supervised task.
- Output layer gets added.
- Global fine tuning by gradient descent on supervised criterion.

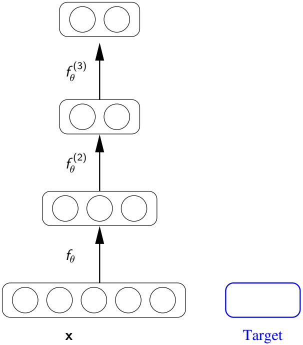

Learning deep networks
Supervised fine-tuning

- Initial deep mapping was learnt in an unsupervised way.
- → initialization for a supervised task.
- Output layer gets added.
- Global fine tuning by gradient descent on supervised criterion.

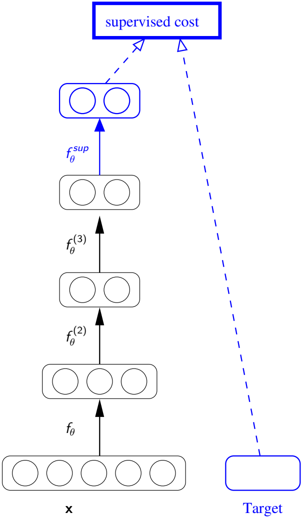

Perspectives on denoising autoencoders
Manifold learning perspective

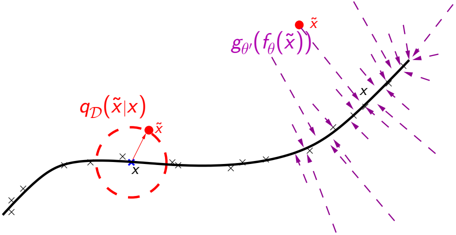

Denoising autoencoder can be seen as a way to learn a manifold:

- Suppose training data ($\times$) concentrate near a low-dimensional manifold.
- Corrupted examples ($\bullet$) are obtained by applying corruption process $q_\mathcal{D}(\widetilde{X}|X)$ and will lie farther from the manifold.
- The model learns with $p(X|\widetilde{X})$ to "project them back" onto the manifold.
- Intermediate representation Y can be interpreted as a coordinate system for points on the manifold.

Perspectives on denoising autoencoders

Information theoretic perspective

- Consider $X \sim q(X)$, q unknown. $\widetilde{X} \sim q_{\mathcal{D}}(\widetilde{X}|X)$. $Y = f_\theta(\widetilde{X})$.
- It can be shown that minimizing the expected reconstruction error amounts to maximizing a lower bound on mutual information $\mathbb{I}(X; Y)$.
- Denoising autoencoder training can thus be justified by the objective that hidden representation Y captures as much information as possible about X *even as Y is a function of corrupted input.*

Perspectives on denoising autoencoders
Generative model perspective

- Denoising autoencoder training can be shown to be equivalent to maximizing a variational bound on the likelihood of a generative model for the corrupted data.

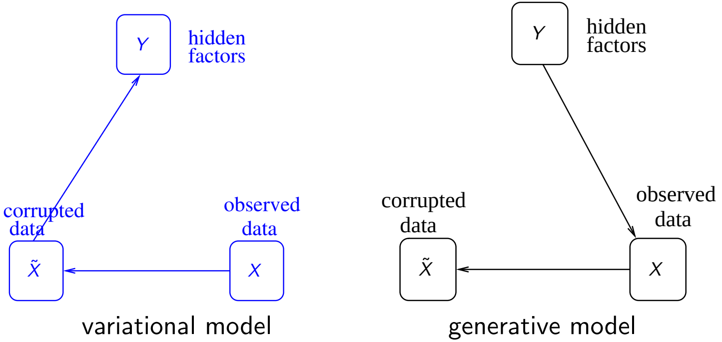

Benchmark problems

Variations on MNIST digit classification

basic: subset of original MNIST digits: 10 000 training samples, 2 000 validation samples, 50 000 test samples.

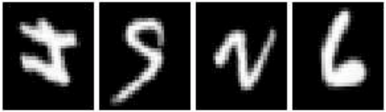

rot: applied random rotation (angle between 0 and 2π radians)

bg-rand: background made of random pixels (value in $0 \dots 255$)

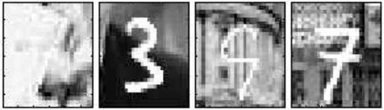

bg-img: background is random patch from one of 20 images

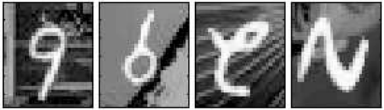

rot-bg-img: combination of rotation and background image

Benchmark problems
Shape discrimination

- **rect:** discriminate between tall and wide rectangles on black background.

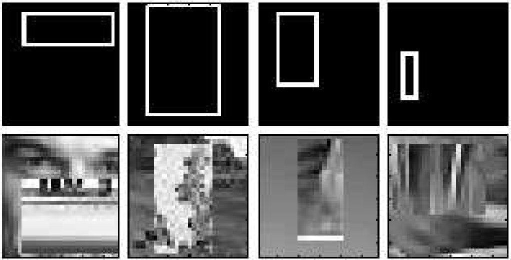

- **rect-img**: borderless rectangle filled with random image patch. Background is a different image patch.
- **convex:** discriminate between convex and non-convex shapes.

Experiments

We compared the following algorithms on the benchmark problems:

- **SVM**$_{rbf}$: suport Vector Machines with Gaussian Kernel.
- **DBN-3**: Deep Belief Nets with 3 hidden layers (stacked Restricted Boltzmann Machines trained with contrastive divergence).
- **SAA-3**: Stacked Autoassociators with 3 hidden layers (no denoising).
- **SdA-3**: Stacked Denoising Autoassociators with 3 hidden layers.

Hyper-parameters for all algorithms were tuned based on classificaiton performance on validation set. (In particular hidden-layer sizes, and ν for **SdA-3**).

Performance comparison
Results

Dataset	SVM_{rbf}	DBN-3	SAA-3	SdA-3 (ν)	$SVM_{rbf}(\nu)$
basic	$3.03_{\pm 0.15}$	$3.11_{\pm 0.15}$	$3.46_{\pm 0.16}$	$2.80_{\pm 0.14}$ (10%)	3.07 (10%)
rot	$11.11_{\pm 0.28}$	$10.30_{\pm 0.27}$	$10.30_{\pm 0.27}$	$10.29_{\pm 0.27}$ (10%)	11.62 (10%)
bg-rand	$14.58_{\pm 0.31}$	$6.73_{\pm 0.22}$	$11.28_{\pm 0.28}$	$10.38_{\pm 0.27}$ (40%)	15.63 (25%)
bg-img	$22.61_{\pm 0.37}$	$16.31_{\pm 0.32}$	$23.00_{\pm 0.37}$	$16.68_{\pm 0.33}$ (25%)	23.15 (25%)
rot-bg-img	$55.18_{\pm 0.44}$	$47.39_{\pm 0.44}$	$51.93_{\pm 0.44}$	$44.49_{\pm 0.44}$ (25%)	54.16 (10%)
rect	$2.15_{\pm 0.13}$	$2.60_{\pm 0.14}$	$2.41_{\pm 0.13}$	$1.99_{\pm 0.12}$ (10%)	2.45 (25%)
rect-img	$24.04_{\pm 0.37}$	$22.50_{\pm 0.37}$	$24.05_{\pm 0.37}$	$21.59_{\pm 0.36}$ (25%)	23.00 (10%)
convex	$19.13_{\pm 0.34}$	$18.63_{\pm 0.34}$	$18.41_{\pm 0.34}$	$19.06_{\pm 0.34}$ (10%)	24.20 (10%)

Performance comparison

Results

Dataset	**SVM$_{rbf}$**	**DBN-3**	**SAA-3**	**SdA-3** (ν)	**SVM$_{rbf}$**(ν)
basic	3.03$\pm$0.15	3.11$\pm$0.15	3.46$\pm$0.16	2.80$\pm$0.14 (10%)	3.07 (10%)
rot	11.11$\pm$0.28	10.30$\pm$0.27	10.30$\pm$0.27	10.29$\pm$0.27 (10%)	11.62 (10%)
bg-rand	14.58$\pm$0.31	6.73$\pm$0.22	11.28$\pm$0.28	10.38$\pm$0.27 (40%)	15.63 (25%)
bg-img	22.61$\pm$0.37	16.31$\pm$0.32	23.00$\pm$0.37	16.68$\pm$0.33 (25%)	23.15 (25%)
rot-bg-img	55.18$\pm$0.44	47.39$\pm$0.44	51.93$\pm$0.44	44.49$\pm$0.44 (25%)	54.16 (10%)
rect	2.15$\pm$0.13	2.60$\pm$0.14	2.41$\pm$0.13	1.99$\pm$0.12 (10%)	2.45 (25%)
rect-img	24.04$\pm$0.37	22.50$\pm$0.37	24.05$\pm$0.37	21.59$\pm$0.36 (25%)	23.00 (10%)
convex	19.13$\pm$0.34	18.63$\pm$0.34	18.41$\pm$0.34	19.06$\pm$0.34 (10%)	24.20 (10%)

Performance comparison
Results

Dataset	SVM_{rbf}	DBN-3	SAA-3	<u>SdA-3</u> (ν)	$SVM_{rbf}(\nu)$
basic	$3.03_{\pm 0.15}$	$3.11_{\pm 0.15}$	$3.46_{\pm 0.16}$	$2.80_{\pm 0.14}$ (10%)	3.07 (10%)
rot	$11.11_{\pm 0.28}$	$10.30_{\pm 0.27}$	$10.30_{\pm 0.27}$	$10.29_{\pm 0.27}$ (10%)	11.62 (10%)
bg-rand	$14.58_{\pm 0.31}$	$6.73_{\pm 0.22}$	$11.28_{\pm 0.28}$	$10.38_{\pm 0.27}$ (40%)	15.63 (25%)
bg-img	$22.61_{\pm 0.37}$	$16.31_{\pm 0.32}$	$23.00_{\pm 0.37}$	$16.68_{\pm 0.33}$ (25%)	23.15 (25%)
rot-bg-img	$55.18_{\pm 0.44}$	$47.39_{\pm 0.44}$	$51.93_{\pm 0.44}$	$44.49_{\pm 0.44}$ (25%)	54.16 (10%)
rect	$2.15_{\pm 0.13}$	$2.60_{\pm 0.14}$	$2.41_{\pm 0.13}$	$1.99_{\pm 0.12}$ (10%)	2.45 (25%)
rect-img	$24.04_{\pm 0.37}$	$22.50_{\pm 0.37}$	$24.05_{\pm 0.37}$	$21.59_{\pm 0.36}$ (25%)	23.00 (10%)
convex	$19.13_{\pm 0.34}$	$18.63_{\pm 0.34}$	$18.41_{\pm 0.34}$	$19.06_{\pm 0.34}$ (10%)	24.20 (10%)

Performance comparison
Results

Dataset	SVM$_{rbf}$	DBN-3	SAA-3	SdA-3 (ν)	SVM$_{rbf}$(ν)
basic	3.03$\pm$0.15	3.11$\pm$0.15	3.46$\pm$0.16	2.80$\pm$0.14 (10%)	3.07 (10%)
rot	11.11$\pm$0.28	10.30$\pm$0.27	10.30$\pm$0.27	10.29$\pm$0.27 (10%)	11.62 (10%)
bg-rand	14.58$\pm$0.31	6.73$\pm$0.22	11.28$\pm$0.28	10.38$\pm$0.27 (40%)	15.63 (25%)
bg-img	22.61$\pm$0.37	16.31$\pm$0.32	23.00$\pm$0.37	16.68$\pm$0.33 (25%)	23.15 (25%)
rot-bg-img	55.18$\pm$0.44	47.39$\pm$0.44	51.93$\pm$0.44	44.49$\pm$0.44 (25%)	54.16 (10%)
rect	2.15$\pm$0.13	2.60$\pm$0.14	2.41$\pm$0.13	1.99$\pm$0.12 (10%)	2.45 (25%)
rect-img	24.04$\pm$0.37	22.50$\pm$0.37	24.05$\pm$0.37	21.59$\pm$0.36 (25%)	23.00 (10%)
convex	19.13$\pm$0.34	18.63$\pm$0.34	18.41$\pm$0.34	19.06$\pm$0.34 (10%)	24.20 (10%)

Performance comparison
Results

Dataset	SVM_{rbf}	DBN-3	SAA-3	SdA-3 (ν)	SVM_{rbf} (ν)
basic	$3.03_{\pm 0.15}$	$3.11_{\pm 0.15}$	$3.46_{\pm 0.16}$	$2.80_{\pm 0.14}$ (10%)	3.07 (10%)
rot	$11.11_{\pm 0.28}$	$10.30_{\pm 0.27}$	$10.30_{\pm 0.27}$	$10.29_{\pm 0.27}$ (10%)	11.62 (10%)
bg-rand	$14.58_{\pm 0.31}$	$6.73_{\pm 0.22}$	$11.28_{\pm 0.28}$	$10.38_{\pm 0.27}$ (40%)	15.63 (25%)
bg-img	$22.61_{\pm 0.37}$	$16.31_{\pm 0.32}$	$23.00_{\pm 0.37}$	$16.68_{\pm 0.33}$ (25%)	23.15 (25%)
rot-bg-img	$55.18_{\pm 0.44}$	$47.39_{\pm 0.44}$	$51.93_{\pm 0.44}$	$44.49_{\pm 0.44}$ (25%)	54.16 (10%)
rect	$2.15_{\pm 0.13}$	$2.60_{\pm 0.14}$	$2.41_{\pm 0.13}$	$1.99_{\pm 0.12}$ (10%)	2.45 (25%)
rect-img	$24.04_{\pm 0.37}$	$22.50_{\pm 0.37}$	$24.05_{\pm 0.37}$	$21.59_{\pm 0.36}$ (25%)	23.00 (10%)
convex	$19.13_{\pm 0.34}$	$18.63_{\pm 0.34}$	$18.41_{\pm 0.34}$	$19.06_{\pm 0.34}$ (10%)	24.20 (10%)

Performance comparison

Results

Dataset	SVM_{rbf}	DBN-3	SAA-3	SdA-3 (ν)	$\text{SVM}_{rbf}(\nu)$
basic	$3.03_{\pm 0.15}$	$3.11_{\pm 0.15}$	$3.46_{\pm 0.16}$	$2.80_{\pm 0.14}$ (10%)	3.07 (10%)
rot	$11.11_{\pm 0.28}$	$10.30_{\pm 0.27}$	$10.30_{\pm 0.27}$	$10.29_{\pm 0.27}$ (10%)	11.62 (10%)
bg-rand	$14.58_{\pm 0.31}$	$6.73_{\pm 0.22}$	$11.28_{\pm 0.28}$	$10.38_{\pm 0.27}$ (40%)	15.63 (25%)
bg-img	$22.61_{\pm 0.37}$	$16.31_{\pm 0.32}$	$23.00_{\pm 0.37}$	$16.68_{\pm 0.33}$ (25%)	23.15 (25%)
rot-bg-img	$55.18_{\pm 0.44}$	$47.39_{\pm 0.44}$	$51.93_{\pm 0.44}$	$44.49_{\pm 0.44}$ (25%)	54.16 (10%)
rect	$2.15_{\pm 0.13}$	$2.60_{\pm 0.14}$	$2.41_{\pm 0.13}$	$1.99_{\pm 0.12}$ (10%)	2.45 (25%)
rect-img	$24.04_{\pm 0.37}$	$22.50_{\pm 0.37}$	$24.05_{\pm 0.37}$	$21.59_{\pm 0.36}$ (25%)	23.00 (10%)
convex	$19.13_{\pm 0.34}$	$18.63_{\pm 0.34}$	$18.41_{\pm 0.34}$	$19.06_{\pm 0.34}$ (10%)	24.20 (10%)

Performance comparison

Results

Dataset	**SVM$_{rbf}$**	**DBN-3**	**SAA-3**	**SdA-3 (ν)**	**SVM$_{rbf}$(ν)**
basic	$3.03_{\pm 0.15}$	$3.11_{\pm 0.15}$	$3.46_{\pm 0.16}$	$2.80_{\pm 0.14}$ (10%)	3.07 (10%)
rot	$11.11_{\pm 0.28}$	$10.30_{\pm 0.27}$	$10.30_{\pm 0.27}$	$10.29_{\pm 0.27}$ (10%)	11.62 (10%)
bg-rand	$14.58_{\pm 0.31}$	$6.73_{\pm 0.22}$	$11.28_{\pm 0.28}$	$10.38_{\pm 0.27}$ (40%)	15.63 (25%)
bg-img	$22.61_{\pm 0.37}$	$16.31_{\pm 0.32}$	$23.00_{\pm 0.37}$	$16.68_{\pm 0.33}$ (25%)	23.15 (25%)
rot-bg-img	$55.18_{\pm 0.44}$	$47.39_{\pm 0.44}$	$51.93_{\pm 0.44}$	$44.49_{\pm 0.44}$ (25%)	54.16 (10%)
rect	$2.15_{\pm 0.13}$	$2.60_{\pm 0.14}$	$2.41_{\pm 0.13}$	$1.99_{\pm 0.12}$ (10%)	2.45 (25%)
rect-img	$24.04_{\pm 0.37}$	$22.50_{\pm 0.37}$	$24.05_{\pm 0.37}$	$21.59_{\pm 0.36}$ (25%)	23.00 (10%)
convex	$19.13_{\pm 0.34}$	$18.63_{\pm 0.34}$	$18.41_{\pm 0.34}$	$19.06_{\pm 0.34}$ (10%)	24.20 (10%)

Performance comparison
Results

Dataset	SVM$_{rbf}$	DBN-3	SAA-3	SdA-3 (ν)	SVM$_{rbf}$(ν)
basic	3.03$\pm$0.15	3.11$\pm$0.15	3.46$\pm$0.16	2.80$\pm$0.14 (10%)	3.07 (10%)
rot	11.11$\pm$0.28	10.30$\pm$0.27	10.30$\pm$0.27	10.29$\pm$0.27 (10%)	11.62 (10%)
bg-rand	14.58$\pm$0.31	6.73$\pm$0.22	11.28$\pm$0.28	10.38$\pm$0.27 (40%)	15.63 (25%)
bg-img	22.61$\pm$0.37	16.31$\pm$0.32	23.00$\pm$0.37	16.68$\pm$0.33 (25%)	23.15 (25%)
rot-bg-img	55.18$\pm$0.44	47.39$\pm$0.44	51.93$\pm$0.44	44.49$\pm$0.44 (25%)	54.16 (10%)
rect	2.15$\pm$0.13	2.60$\pm$0.14	2.41$\pm$0.13	1.99$\pm$0.12 (10%)	2.45 (25%)
rect-img	24.04$\pm$0.37	22.50$\pm$0.37	24.05$\pm$0.37	21.59$\pm$0.36 (25%)	23.00 (10%)
convex	19.13$\pm$0.34	18.63$\pm$0.34	18.41$\pm$0.34	19.06$\pm$0.34 (10%)	24.20 (10%)

Learnt filters
0 % destroyed

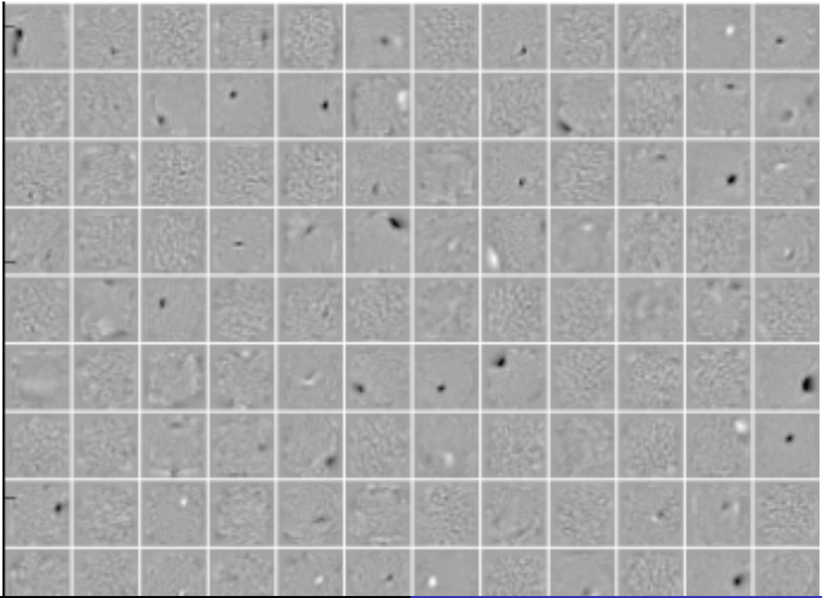

Learnt filters
10 % destroyed

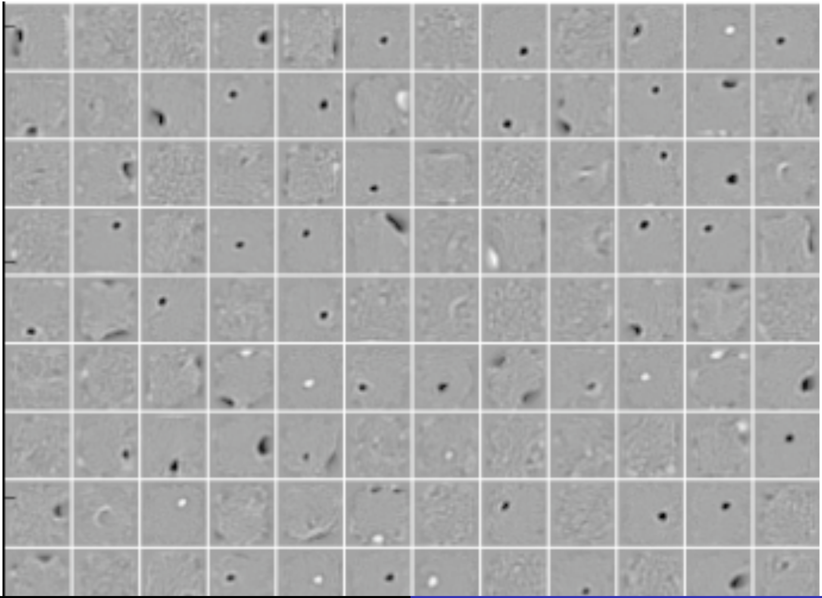

Learnt filters
25 % destroyed

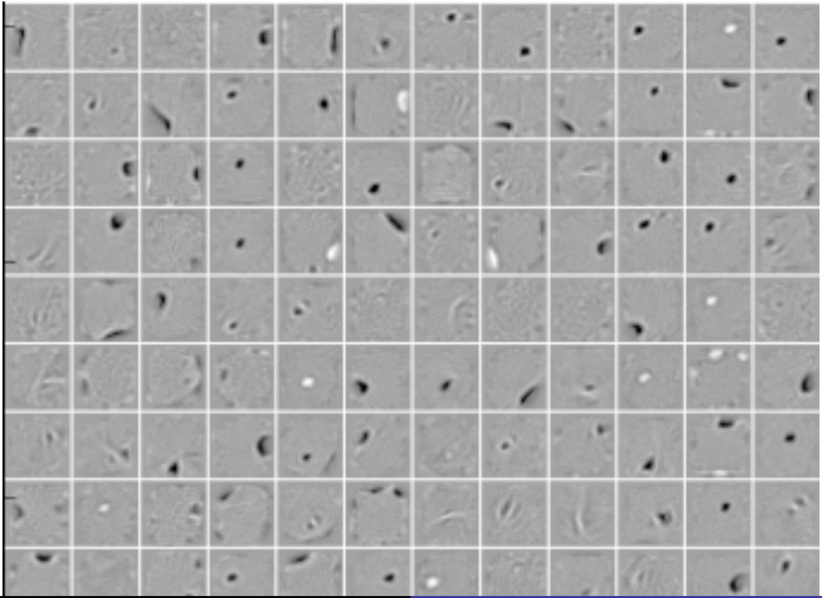

Learnt filters
50 % destroyed

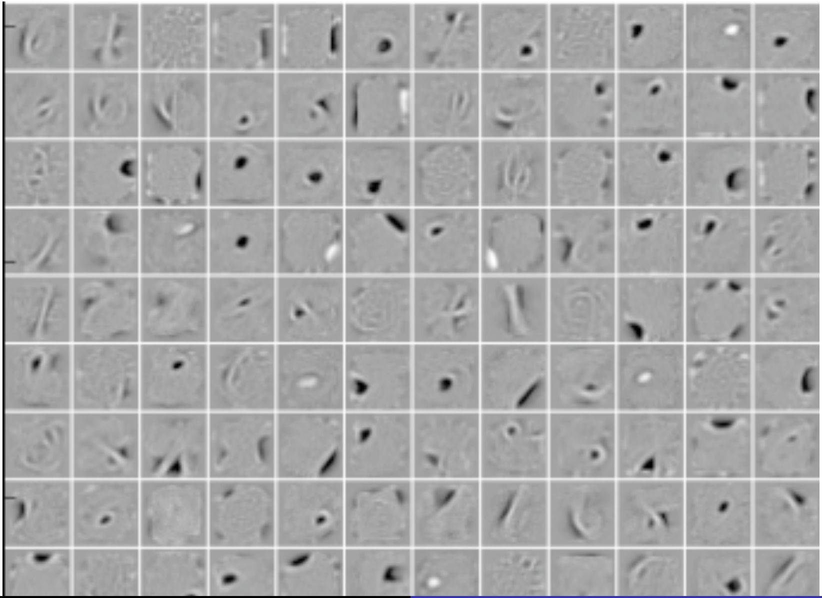

Conclusion and future work

- Unsupervised initialization of layers with an explicit denoising criterion appears to help capture interesting structure in the input distribution.
- This leads to intermediate representations much better suited for subsequent learning tasks such as supervised classification.
- Resulting algorithm for learning deep networks is simple and improves on state-of-the-art on benchmark problems.
- Although our experimental focus was supervised classification, **SdA** is directly usable in a semi-supervised setting.
- Future work will investigate the effect of different types of corruption process.

THANK YOU!

Performance comparison

Dataset	SVM_{rbf}	SVM_{poly}	DBN-1	DBN-3	SAA-3	SdA-3 (ν)
basic	3.03$\pm$0.15	3.69$\pm$0.17	3.94$\pm$0.17	3.11$\pm$0.15	3.46$\pm$0.16	2.80$\pm$0.14 (10%)
rot	11.11$\pm$0.28	15.42$\pm$0.32	14.69$\pm$0.31	10.30$\pm$0.27	10.30$\pm$0.27	10.29$\pm$0.27 (10%)
bg-rand	14.58$\pm$0.31	16.62$\pm$0.33	9.80$\pm$0.26	6.73$\pm$0.22	11.28$\pm$0.28	10.38$\pm$0.27 (40%)
bg-img	22.61$\pm$0.37	24.01$\pm$0.37	16.15$\pm$0.32	16.31$\pm$0.32	23.00$\pm$0.37	16.68$\pm$0.33 (25%)
rot-bg-img	55.18$\pm$0.44	56.41$\pm$0.43	52.21$\pm$0.44	47.39$\pm$0.44	51.93$\pm$0.44	44.49$\pm$0.44 (25%)
rect	2.15$\pm$0.13	2.15$\pm$0.13	4.71$\pm$0.19	2.60$\pm$0.14	2.41$\pm$0.13	1.99$\pm$0.12 (10%)
rect-img	24.04$\pm$0.37	24.05$\pm$0.37	23.69$\pm$0.37	22.50$\pm$0.37	24.05$\pm$0.37	21.59$\pm$0.36 (25%)
convex	19.13$\pm$0.34	19.82$\pm$0.35	19.92$\pm$0.35	18.63$\pm$0.34	18.41$\pm$0.34	19.06$\pm$0.34 (10%)

red when confidence intervals overlap.

References

Bengio, Y., Lamblin, P., Popovici, D., and Larochelle, H. (2007).
Greedy layer-wise training of deep networks.
In *NIPS 19*.

Gallinari, P., LeCun, Y., Thiria, S., and Fogelman-Soulie, F. (1987).
Memoires associatives distribuees.
In *Proceedings of COGNITIVA 87*, Paris, La Villette.

Hinton, G. E., Osindero, S., and Teh, Y. (2006).
A fast learning algorithm for deep belief nets.
Neural Computation, 18:1527–1554.

Hopfield, J. J. (1982).
Neural networks and physical systems with emergent collective computational abilities.
Proceedings of the National Academy of Sciences, USA, 79.

LeCun, Y. (1987).
Modèles connexionistes de l'apprentissage.
PhD thesis, Université de Paris VI.

Ranzato, M., Poultney, C., Chopra, S., and LeCun, Y. (2007).

Efficient learning of sparse representations with an energy-based model.

In et al., J. P., editor, *Advances in Neural Information Processing Systems (NIPS 2006)*. MIT Press.

Rumelhart, D. E., Hinton, G. E., and Williams, R. J. (1986).

Learning representations by back-propagating errors.

Nature, 323:533–536.